

THE HYDROGEN IDENTITY FOR LAPLACIANS

OLIVER KNILL

ABSTRACT. For any 1-dimensional simplicial complex G defined by a finite simple graph, the hydrogen identity $|H| = L - L^{-1}$ holds, where $|H| = (|d| + |d|^*)^2$ is the sign-less Hodge Laplacian defined by the sign-less incidence matrix $|d|$ and where L is the connection Laplacian. Having linked the Laplacian spectral radius ρ of G with the spectral radius of the adjacency matrix its connection graph G' allows for every k to estimate $\rho \leq r_k - 1/r_k$, where $r_k = 1 + (P(k))^{1/k}$ and $P(k) = \max_x P(k, x)$, where $P(k, x)$ is the number of paths of length k starting at a vertex x in G' . The limit $r_k - 1/r_k$ for $k \rightarrow \infty$ is the spectral radius ρ of $|H|$ which by Wielandt is an upper bound for the spectral radius ρ of $H = (d + d^*)^2$, with equality if G is bipartite. We can relate so the growth rate of the random walks in the line graph G_L of G with the one in the connection graph G' of G . The hydrogen identity implies that the random walk $\psi(n) = L^n \psi$ on the connection graph G' with integer n solves the 1-dimensional Jacobi equation $\Delta \psi = |H|^2 \psi$ with $\Delta u(n) = u(n+2) - 2u(n) + u(n-2)$ and assures that every solution is represented by such a reversible path integral. The hydrogen identity also holds over any finite field F . There, the dynamics $L^n \psi$ with $n \in \mathbb{Z}$ is a reversible cellular automaton with alphabet F^G . By taking products of simplicial complexes, such processes can be defined over any lattice \mathbb{Z}^r . Since L^2 and L^{-2} are isospectral, by a theorem of Kirby, L^2 is always similar to a symplectic matrix if the graph has an even number of simplices. By the implicit function theorem, the hydrogen relation is robust in the following sense: any matrix K close to $|H|$ with the same support than $|H|$ can still be written as $K = L - L^{-1}$ with a connection Laplacian satisfying $L(x, y) = L^{-1}(x, y) = 0$ if $x \cap y = \emptyset$.

1. INTRODUCTION

1.1. The largest eigenvalue ρ of the Kirchhoff graph Laplacian H_0 of a graph G depends in an intricate way on the vertex degrees of G . Quite a few estimates for the spectral radius ρ are known [25, 7, 30, 4, 8,

Date: March 4, 2018.

1991 Mathematics Subject Classification. 11P32, 11R52, 11A41.

Key words and phrases. Graph Laplacian, Spectral radius, Connection Laplacian, graphs.

27, 19, 20, 31]. These estimates often use maximal local vertex degree quantities which are random walk related. We look at the problem by relating the Hodge Laplacian $H = H_0 \oplus H_1$ with an adjacency matrix A of a connection graph G' defined by G . This allows to use estimates for the later, like [2, 28, 29] or random cases [18] to get estimates for the graph Laplacian. The adjacency spectral radius $r(G)$ is accessible through random walk estimates and therefore has monotonicity properties like $r(A) \leq r(B)$ if A is a subgraph of B . While the spectrum of the Kirchoff Laplacian H_0 has already been analyzed with the help of the line graph, an idea going back at least to [1], the hydrogen relation $L - L^{-1} = |H|$ considered here is an other link.

1.2. Adjacency matrices are more pleasant for estimates than Laplacians because they are 0 – 1 matrices and so non-negative. As the spectral radius of an adjacency matrix A is a Lyapunov exponent which can be estimated as $\rho(A) \leq \rho(A^k)^{1/k} \leq (P(k))^{1/k}$, where $P(k)$ is the number of paths of length k in the corresponding graph, one can get various estimates by picking a fixed k and go about estimating the maximal number of paths of length k starting at some point. Already the simplest estimates for A leads to effective estimate ρ , especially for Barycentric refinements, where $\rho = (d + 3) - (d + 3)^{-1}$ where d is the maximal vertex degree. In general, we get in the simplest case $\rho \leq r - 1/r$, where r is 1 plus the maximal of the sum of a pair vertex degrees of adjacent vertices. Global estimates like [2, 28] for adjacency matrices lead to other upper bounds. Because the spectrum of L has negative parts, the Schur inequality discussed below can be useful too. It produces insight about the spectrum of L and so about the spectrum of $|H|$.

1.3. For a finite abstract simplicial complex G - a finite set of non-empty sets closed under the operation of taking non-empty subsets - the connection Laplacian L is defined by the properties $L(x, y) = 1$ if $x \cap y$ intersect and $L(x, y) = 0$ if $x \cap y = \emptyset$. The matrix L is the Fredholm matrix $L = \mathbf{1} + A$ for the adjacency matrix A of the connection graph G' and has remarkable properties. First of all, it is always unimodular. Then, the sum of the matrix entries of the inverse L^{-1} is the Euler characteristic $\chi(G)$ of G . One can also write $\chi(G) = p(G) - n(G)$, where $p(G)$ are the positive and $n(G)$ are the negative eigenvalues of L [14]. Finally, the matrix entries $g(x, y)$ of the inverse $g = L^{-1}$ can be given explicitly as $\omega(x)\omega(y)\chi(\text{St}(x) \cap \text{St}(y))$, where $\text{St}(x) = \{y \supset x \mid y \in G\}$ is the star of x and $\omega(x) = (-1)^{\dim(x)}$ [17].

1.4. In the case of a 1-dimensional complex, G enjoys more properties: the spectrum of the square L^2 satisfies the symmetry $\sigma(L^2) = 1/\sigma(L^2)$. This relation indicates already that L is of symplectic nature. It is equivalent to a functional equation $\zeta(s) = \zeta(-s)$ for the zeta function associated to L [16]. The hydrogen operator $L - L^{-1}$ was of interest to us at first as its trace is a Dehn-Sommerville type quantity $\sum_x \chi(S(x))$ [13], where $S(x)$ is the unit sphere of a vertex x in the Barycentric refinement graph. It is zero for nice triangulations of even dimensional manifolds. The main point we make here is that in one dimensions, $L - L^{-1}$ always is the sign-less Hodge operator $|H| = (|d| + |d|)^*$, where $|d|$ is the sign-less gradient. For bipartite graphs, the sign-less Hodge operator $|H|$ is conjugated to the usual Hodge operator H . In [14], we have looked at the hydrogen relation only in the case of graphs which were Barycentric refinements and so bipartite which implied $|H|$ to be conjugated to H .

2. THE HYDROGEN RELATION

2.1. The Kirchhoff Laplacian H_0 of a graph G with v vertices is the $v \times v$ matrix $H = B - A$, where B is the diagonal vertex degree matrix and A is the adjacency matrix of G . The relation $d_0 f((x, y)) = f(y) - f(x)$ defines an incidence matrix d which is defined, once an orientation has been chosen on the edge set E . The choice of orientation does not affect H , nor the spectrum of $D = d + d^*$. The matrix d_0 is a $e \times v$ matrix, where e is the number of edges of G . It defines naturally a $(e+v) \times (e+v)$ matrix d and so $D = d + d^*$ with $D^2 = H$. The matrix H_0 can now be rewritten as $H_0 = d_0^* d_0$. It is so the discrete analogue of $\Delta = \text{div} \circ \text{grad}$ in calculus. If we look at the sign-less derivative $|d_0|$, which is a 0-1 matrix, then still $|d_0|^2 = 0$ in one dimensions and $|H| = (|d| + |d|^*)^2 = |H_0| \oplus |H_1|$ is the sign-less Laplacian. Unlike H_0 , which always has an eigenvalue 0, the sign-less Kirchhoff matrix $|H_0|$ is invertible if the graph G is not bipartite.

2.2. The Barycentric refinement G_1 of a finite simple graph $G = (V, E)$ is a new graph Γ with vertex set $V_1 = V \cup E$ and where a pair $(a, b) \in V \times E$ is in the edge set E_1 if $a \subset b$. If v is the cardinality of V and e is the cardinality of E , then $\chi(G) = v - e$ is the Euler characteristic of G . The new graph Γ has $n = v + e$ vertices and $m = \sum_v \text{deg}(v) = 2e$ edges. The invariance of Euler characteristic under Barycentric refinements is in 1-dimensions just the Euler handshake formula. The Euler characteristic $\chi(G)$ of a simplicial complex G is in general (not necessarily 1-dimensional case) an invariant as the

f -vector $f = (v, e, \dots)$ of a complex is explicitly mapped to a new vector Sf for the matrix S which has $(1, -1, 1, \dots)$ as eigenvalues of A^T . The matrix S is upper triangular and given by $S_{ij} = i!S(j, i)$, where $S(j, i)$ are **Stirling numbers** of the second kind.

2.3. The 1-form Laplacian $H_1 = dd^*$ defined by the $v \times e$ matrix d has the same non-zero spectrum than $H_0 = d^*d$. This super symmetry relation between the 1-form Laplacian H_1 and 0-form Laplacian H_0 appears have been used first in [1]. The nullity of H_0 is the genus b_1 while the nullity of H_1 is b_0 the number of connected components of G . The Euler characteristic $\chi = v - e$ satisfies the Euler-Poincaré formula $b_0 - b_1$. The Dirac matrix $D = d + d^*$ is a $n \times n$ matrix with $n = v + e$. It defines $H = D^2$. Because $d^2 = (d^*)^2 = 0$, we have $D^2 = d^*d + dd^*$ so that $H = H_0 \oplus H_1$ decomposes into two blocks. If we take the absolute values of all entries, we end up with the sign-less Hodge Laplacian $|H| = (|d| + |d^*|)^2 = |d||d^*| + |d^*||d|$.

2.4. The connection matrix of G is $L(x, y) = 1$ if $x \cap y \neq \emptyset$ and $L(x, y) = 0$ if $x \cap y = \emptyset$. For 1-dimensional complexes G , L is a $(v + e) \times (v + e)$ matrix. It has the same size than the Hodge operator H or its sign-less Hodge matrix $|H|$. But unlike H or $|H|$, the matrix L is always invertible and its inverse L^{-1} is always integer-valued. Also, unlike the Hodge matrix H , which is reducible, the matrix L is always irreducible if G is connected. The reason for this ergodicity property is that L is a non-negative matrix and that L^n is a positive matrix for large enough n as one can see when looking at a random walk interpretation: the matrix is the adjacency matrix of the graph G' for which loops have been attached to each vertex x .

Theorem 1 (Hydrogen relation). *For any finite simple graph, $|H| = L - L^{-1}$.*

Proof. While we have already seen this in [17], we have looked there only at the situation when H and $|H|$ were similar. The proof of the hydrogen relation is in the 1-dimensional case especially simple, as we can explicitly write down the entries of the inverse L^{-1} . We have $(L - L^{-1})(x) = \chi(S(x)) = \deg(x)$ where $\deg(x)$ is the vertex degree of the Barycentric refinement. The Euler characteristic $\chi(S(x))$ of the unit sphere $S(x)$ is equal to the vertex degree of an original vertex x and equal to 2 for an edge, because an edge only has two neighbors provided that G is 1-dimensional. If x is vertex and y an edge containing x , then $L(x, y) = 1$ and $L^{-1}(x, y) = 1$. If x, y are vertices, then $L(x, y) = 0$ and $L^{-1}(x, y) = -1$. If x, y are edges, then $L(x, y) = 1$ and $L^{-1}(x, y) = 0$. \square

2.5. The name “hydrogen” had originally been chosen because the Laplacian $L = -\Delta/(4\pi)$ in Euclidean space has an inverse with a kernel $1/|x - y|$ of the potential of the hydrogen atom. While the Laplacian in R^3 is not invertible, the integral operator L^{-1} allows formally to see $L - L^{-1}$ as a quantum mechanical system, where at each point of space, a “charge” is located. We can think of the Laplacian L itself as a kinetic, and the “integral operator” L^{-1} as a potential theoretic component of H . This is a reason also why for the invertible connection Laplacian L , the inverse entries $g(x, y)$, the Green’s functions, has an interpretation as a potential energy between two simplices x, y .

2.6. The energy theorem

$$\sum_x \sum_y g(x, y) = \chi(G)$$

which holds for an arbitrary simplicial complex, then suggests to see the Euler characteristic as a “total potential energy”. The kinetic operator L is unitary conjugated to an operator M for which the sum $\sum_x \sum_y M(x, y) = \omega(G)$ is the Wu characteristic. As it involves pairs of intersecting simplices, the Wu characteristic can be seen as a potential theoretic part and Euler characteristic as kinetic energy. The hydrogen relation combines the kinetic and potential theoretic part. For locally Euclidean complexes, for which Poincaré duality holds, the two energies balance out and the total energy is zero. For structures with boundary, the energy (the curvature of the valuation) is supported on the boundary, similarly as the charge equilibria of Riesz measures are supported on the boundary of regions in potential theory.

2.7. Since for every connected graph, the operator L is irreducible with a unique Perron-Frobenius eigenvalue, this is also inherited by the sign-less Hodge operator $|H|$. The corresponding eigenvalue has no sign changes. Now, the maximal eigenvalue can only become smaller if $|H|$ is replaced by H .

Corollary 1 (Relating Hodge and Adjacency). *The spectral radius ρ of H is bounded above by $r - 1/r$, where r is the spectral radius of L .*

Proof. From the hydrogen relation, we only get the spectral radius $\rho(|H|) = r - 1/r$. But as $|H|$ is a dominating matrix for H , a result of Wielandt ([22], Chapter 2.2, Theorem 2.1), assures that the maximal eigenvalue of H is smaller or equal than the maximal eigenvalue of $|H|$. \square

2.8. Since $L = 1 + A$ with adjacency matrix A for G' , we can estimate ρ in terms of the eigenvalues of A . L is a non-negative matrix as it only has entries 0 or 1. If G is a Barycentric refinement of a complex, we can estimate the largest eigenvalue of L as the maximal row sum. In the case of a refined graph where every edge is connected to a vertex with only 2 neighbors, we get the two vertex degree $d + 2$, where d is the maximal vertex degree of G . Therefore, the connection Laplacian spectral radius can be estimated from above by $d + 3$. If G is a Barycentric refinement we have then

$$\rho \leq (d + 3) - 1/(d + 3) .$$

We can do better by incorporating also neighboring vertex degrees. Still, already here, the estimate in [1] is better, as the maximal row sum in the 1-form Laplacian is then $2 + (d_x - 1) + 1 = d_x + 2$. The Anderson-Morely estimates gives for Barycentric refined graphs

$$\rho \leq d + 2 .$$

2.9. Examples:

1) For a star graph $S(n)$, where a single vertex has degree n , the spectral radius of H is $n + 1$. For $n = 4$, where the $S(4)$ has spectral radius 5, the Barycentric refinement has spectral radius 5.30278. The estimate $d + 3 - 1/(d + 3) = 7 - 1/7 = 6.85714$ is less effective than the estimate using neighboring vertex degrees.

2) For the circular graph $C(2n)$ the spectral radius is 4 for all n . As $2n$ is even, they are Barycentric refinements. The above estimate gives $5 - 1/5 = 4.8$ independent of n . This is a regular graph for which the estimate in [20] does not apply.

3) For a linear graph $L(2n + 1)$ we always get the estimate $5 - 1/5$, the same estimate as for circular graph. The spectral radius is 3 for $n = 1$ and increases monotonically to 4 for $n \rightarrow \infty$. For $n = 1$, the dual vertex spectral estimate gives 3.75 which is better than the Brualdi-Hoffmann-Stanley estimate 3.4314 or [20] which gives 3.9333. However, for larger $n > 1$, the estimate [20] is the best. There are estimates $2d - 2/((2l + 1)n)$ ([27] Theorem 3.5) or $2d - 1/(ln)$ ([20] Theorem 2.3) for irregular graphs of diameter l and n vertices. We see that there are cases, where the estimate does not even beat the trivial estimate $2d$.

4) For the complete graphs K_2, K_3 , the global estimates [2, 28] are best.

2.10. We also get:

Corollary 2 (Adjacency estimate). *For any finite simple graph $G = (V, E)$, the spectral radius estimate $\rho \leq 1 + r - 1/(1 + r)$ holds, where r is the maximum eigenvalue the adjacency matrix of G' .*

Proof. This follows immediately from the hydrogen relation. □

2.11. The simplest estimate is when r is the maximum of $d_x + d_y$ over all pairs $(x, y) \in E$. This is a bit higher than the Anderson-Morely estimate [1], who gave $\rho \leq r$ with $r = \max_{(x,y) \in E} (d_x + d_y)$. Their proof of 1985 which only used the maximal row sum in the 1-form Laplacian. (That article acknowledges H.P. McKean for posing the problem and uses that d^*d and dd^* are essentially isospectral, which is a special case of McKean-Singer super symmetry). In [21], the upper bound $2 + \sqrt{(d_x - 2)(d_y - 2)}$ is given and [30] state $r = \max(d_x + \sqrt{d_x m_x})$, where m_x is the average neighboring degree of x . More estimates are given in [6]. We can improve such bound by looking at paths of length 2. But such estimates are not pretty. The statement allows for any estimate on the maximal eigenvalue of the adjacency matrix A of G' gives and a spectral estimate of the Laplacian H_0 . Better is the estimate $r \leq 1 + \max_i (1/r_i) \sum_j A_{ij} r_j$, where r_j is the row sum of the adjacency matrix which is bounded above by $d_x + d_y$.

2.12. Global estimates are still often better in highly saturated graphs, where pairs of vertices where the maximal vertex degree exist. The estimates through L are good if the maximum is attained at not-adjacent places. Considerable work was done already to improve the trivial upper bound $\rho \leq 2d$ which just estimates the row sums of $|H|$ and so gives a bound for $\rho(H)$. In principle, one can get arbitrary close to the spectral radius of $|H|$. Let $P(k, x)$ denote the number of paths of length k in the connection graph G' starting at x . The spectral radius of L can be estimated by $r_k = 1 + \max_x P(k, x)$.

Corollary 3 (Random walk estimate). *For any k , $\rho \leq r_k - 1/r_k$.*

2.13. One can so estimate the spectral radius of $|H|$ arbitrary well. To make it effective and geometric, one would have to estimate $P(k, x)$ in terms of the local geometry of the graph. In the bipartite case, these estimates become sharp for H even at least in the limit $k \rightarrow \infty$. In any case, we see that we can estimate the spectral radius of a graph Laplacian of a graph G dynamically by the growth rate of random walks in a related connection graph G' . It would be nice to exploit this for Erdős-Renyi graphs. It is reasonable as the upper bound estimates depend on the clustering of a large number of large vertex degrees,

SPECTRAL RADIUS

leading to a high number $P(k, x)$ of paths of length k starting from a point x .

2.14. If G is connected, the maximal eigenvalue of the sign-less Kirchhoff matrix $|H_0|$ is unique. The reason is that $|H_0|$ is a non-negative matrix which for some power m satisfies is a positive matrix $|H_0|^m$ having a unique maximal eigenvalue by the Perron-Frobenius theorem. The classical Kirchhoff matrix H_0 itself can have multiple maximal eigenvalues. For the complete graph K_n for example, the maximal eigenvalue n of H_0 appears with multiplicity $n - 1$, while $|H_0|$ has only a single maximal eigenvalue $2n - 2$ and a single eigenvalue 0. All other $n - 1$ eigenvalues are equal to $n - 2$.

2.15. Here are the matrices written out.

$$L = \begin{bmatrix} 1 & 0 & 0 & 0 & 0 & 0 & 0 & 1 & 1 & 0 & 0 & 0 & 0 & 0 & 0 \\ 0 & 1 & 0 & 0 & 0 & 0 & 0 & 1 & 0 & 1 & 1 & 1 & 0 & 0 & 0 \\ 0 & 0 & 1 & 0 & 0 & 0 & 0 & 0 & 0 & 1 & 0 & 0 & 1 & 0 & 0 \\ 0 & 0 & 0 & 1 & 0 & 0 & 0 & 0 & 1 & 0 & 0 & 0 & 1 & 0 & 0 \\ 0 & 0 & 0 & 0 & 1 & 0 & 0 & 0 & 0 & 0 & 1 & 0 & 0 & 1 & 0 \\ 0 & 0 & 0 & 0 & 0 & 1 & 0 & 0 & 0 & 0 & 0 & 0 & 0 & 1 & 1 \\ 0 & 0 & 0 & 0 & 0 & 0 & 1 & 0 & 0 & 0 & 0 & 1 & 0 & 0 & 1 \\ 1 & 1 & 0 & 0 & 0 & 0 & 0 & 1 & 1 & 1 & 1 & 1 & 0 & 0 & 0 \\ 1 & 0 & 0 & 1 & 0 & 0 & 0 & 1 & 1 & 0 & 0 & 0 & 1 & 0 & 0 \\ 0 & 1 & 1 & 0 & 0 & 0 & 0 & 1 & 0 & 1 & 1 & 1 & 1 & 0 & 0 \\ 0 & 1 & 0 & 0 & 1 & 0 & 0 & 1 & 0 & 1 & 1 & 1 & 0 & 1 & 0 \\ 0 & 1 & 0 & 0 & 0 & 0 & 1 & 1 & 0 & 1 & 1 & 1 & 0 & 0 & 1 \\ 0 & 0 & 1 & 1 & 0 & 0 & 0 & 1 & 1 & 0 & 0 & 1 & 0 & 0 & 0 \\ 0 & 0 & 0 & 0 & 1 & 1 & 0 & 0 & 0 & 0 & 1 & 0 & 0 & 1 & 1 \\ 0 & 0 & 0 & 0 & 0 & 1 & 1 & 0 & 0 & 0 & 0 & 1 & 0 & 1 & 1 \end{bmatrix}$$

$$L^{-1} = \begin{bmatrix} -1 & -1 & 0 & -1 & 0 & 0 & 0 & 1 & 1 & 0 & 0 & 0 & 0 & 0 & 0 \\ -1 & -3 & -1 & 0 & -1 & 0 & -1 & 1 & 0 & 1 & 1 & 1 & 0 & 0 & 0 \\ 0 & -1 & -1 & -1 & 0 & 0 & 0 & 0 & 0 & 1 & 0 & 0 & 1 & 0 & 0 \\ -1 & 0 & -1 & -1 & 0 & 0 & 0 & 0 & 1 & 0 & 0 & 0 & 1 & 0 & 0 \\ 0 & -1 & 0 & 0 & -1 & -1 & 0 & 0 & 0 & 0 & 1 & 0 & 0 & 1 & 0 \\ 0 & 0 & 0 & 0 & -1 & -1 & -1 & 0 & 0 & 0 & 0 & 0 & 0 & 1 & 1 \\ 0 & -1 & 0 & 0 & 0 & -1 & -1 & 0 & 0 & 0 & 0 & 1 & 0 & 0 & 1 \\ 1 & 1 & 0 & 0 & 0 & 0 & 0 & -1 & 0 & 0 & 0 & 0 & 0 & 0 & 0 \\ 1 & 0 & 0 & 1 & 0 & 0 & 0 & 0 & -1 & 0 & 0 & 0 & 0 & 0 & 0 \\ 0 & 1 & 1 & 0 & 0 & 0 & 0 & 0 & 0 & -1 & 0 & 0 & 0 & 0 & 0 \\ 0 & 1 & 0 & 0 & 1 & 0 & 0 & 0 & 0 & 0 & -1 & 0 & 0 & 0 & 0 \\ 0 & 1 & 0 & 0 & 0 & 0 & 1 & 0 & 0 & 0 & 0 & -1 & 0 & 0 & 0 \\ 0 & 0 & 1 & 1 & 0 & 0 & 0 & 0 & 0 & 0 & 0 & 0 & -1 & 0 & 0 \\ 0 & 0 & 0 & 0 & 1 & 1 & 0 & 0 & 0 & 0 & 0 & 0 & 0 & -1 & 0 \\ 0 & 0 & 0 & 0 & 0 & 1 & 1 & 0 & 0 & 0 & 0 & 0 & 0 & 0 & -1 \end{bmatrix}$$

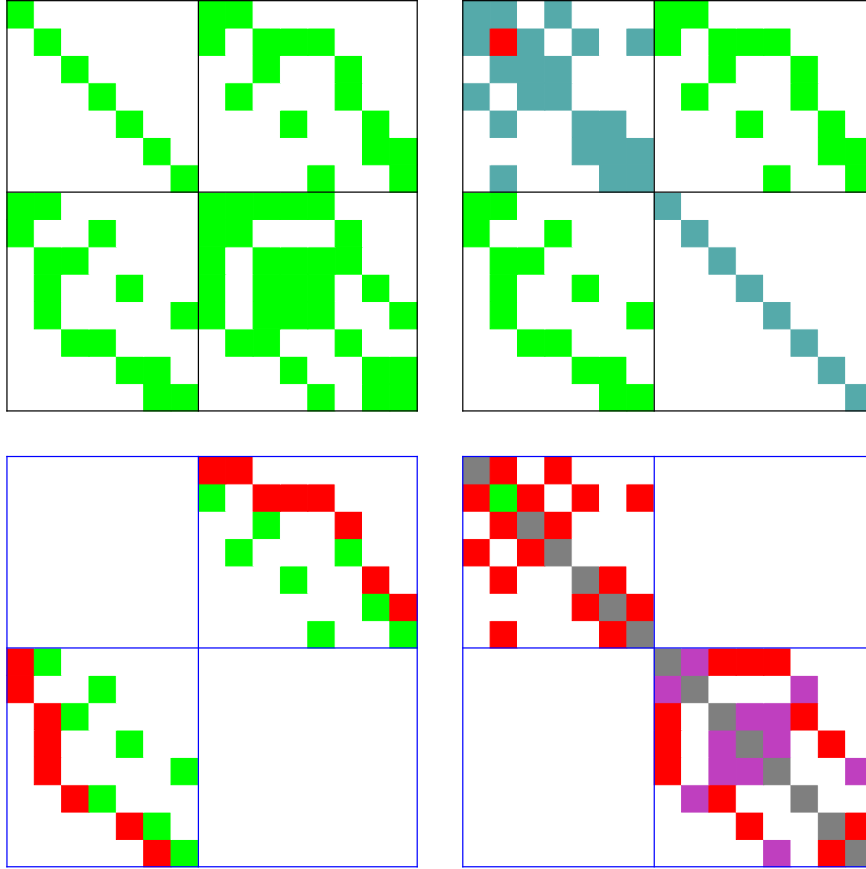


FIGURE 1. We see the connection Laplacian L , its inverse $g = L^{-1}$, the Dirac operator $D = d + d^*$ and the Hodge Laplacian $H = D^2$ for the Barycentric refined figure 8-graph. The hydrogen identity is $|H| = L - g$. In this case we know that H is isospectral to $L - g$.

$$D = \begin{bmatrix} 0 & 0 & 0 & 0 & 0 & 0 & 0 & -1 & -1 & 0 & 0 & 0 & 0 & 0 & 0 \\ 0 & 0 & 0 & 0 & 0 & 0 & 0 & 1 & 0 & -1 & -1 & -1 & 0 & 0 & 0 \\ 0 & 0 & 0 & 0 & 0 & 0 & 0 & 0 & 0 & 1 & 0 & 0 & -1 & 0 & 0 \\ 0 & 0 & 0 & 0 & 0 & 0 & 0 & 0 & 0 & 1 & 0 & 0 & 0 & 1 & 0 \\ 0 & 0 & 0 & 0 & 0 & 0 & 0 & 0 & 0 & 0 & 1 & 0 & 0 & 0 & -1 \\ 0 & 0 & 0 & 0 & 0 & 0 & 0 & 0 & 0 & 0 & 0 & 0 & 1 & 0 & 0 \\ 0 & 0 & 0 & 0 & 0 & 0 & 0 & 0 & 0 & 0 & 0 & 0 & 1 & 0 & 0 \\ -1 & 1 & 0 & 0 & 0 & 0 & 0 & 0 & 0 & 0 & 0 & 0 & 0 & 0 & 0 \\ -1 & 0 & 0 & 1 & 0 & 0 & 0 & 0 & 0 & 0 & 0 & 0 & 0 & 0 & 0 \\ 0 & -1 & 1 & 0 & 0 & 0 & 0 & 0 & 0 & 0 & 0 & 0 & 0 & 0 & 0 \\ 0 & -1 & 0 & 0 & 1 & 0 & 0 & 0 & 0 & 0 & 0 & 0 & 0 & 0 & 0 \\ 0 & -1 & 0 & 0 & 0 & 0 & 1 & 0 & 0 & 0 & 0 & 0 & 0 & 0 & 0 \\ 0 & 0 & -1 & 1 & 0 & 0 & 0 & 0 & 0 & 0 & 0 & 0 & 0 & 0 & 0 \\ 0 & 0 & 0 & 0 & -1 & 1 & 0 & 0 & 0 & 0 & 0 & 0 & 0 & 0 & 0 \\ 0 & 0 & 0 & 0 & 0 & -1 & 1 & 0 & 0 & 0 & 0 & 0 & 0 & 0 & 0 \end{bmatrix}$$

SPECTRAL RADIUS

$$H = D^2 = \begin{bmatrix} 2 & -1 & 0 & -1 & 0 & 0 & 0 & 0 & 0 & 0 & 0 & 0 & 0 & 0 & 0 \\ -1 & 4 & -1 & 0 & -1 & 0 & -1 & 0 & 0 & 0 & 0 & 0 & 0 & 0 & 0 \\ 0 & -1 & 2 & -1 & 0 & 0 & 0 & 0 & 0 & 0 & 0 & 0 & 0 & 0 & 0 \\ -1 & 0 & -1 & 2 & 0 & 0 & 0 & 0 & 0 & 0 & 0 & 0 & 0 & 0 & 0 \\ 0 & -1 & 0 & 0 & 2 & -1 & 0 & 0 & 0 & 0 & 0 & 0 & 0 & 0 & 0 \\ 0 & 0 & 0 & 0 & -1 & 2 & -1 & 0 & 0 & 0 & 0 & 0 & 0 & 0 & 0 \\ 0 & -1 & 0 & 0 & 0 & -1 & 2 & 0 & 0 & 0 & 0 & 0 & 0 & 0 & 0 \\ 0 & 0 & 0 & 0 & 0 & 0 & 0 & 2 & 1 & -1 & -1 & -1 & 0 & 0 & 0 \\ 0 & 0 & 0 & 0 & 0 & 0 & 0 & 1 & 2 & 0 & 0 & 0 & 1 & 0 & 0 \\ 0 & 0 & 0 & 0 & 0 & 0 & 0 & -1 & 0 & 2 & 1 & 1 & -1 & 0 & 0 \\ 0 & 0 & 0 & 0 & 0 & 0 & 0 & -1 & 0 & 1 & 2 & 1 & 0 & -1 & 0 \\ 0 & 0 & 0 & 0 & 0 & 0 & 0 & -1 & 0 & 1 & 1 & 2 & 0 & 0 & 1 \\ 0 & 0 & 0 & 0 & 0 & 0 & 0 & 0 & 1 & -1 & 0 & 0 & 2 & 0 & 0 \\ 0 & 0 & 0 & 0 & 0 & 0 & 0 & 0 & 0 & 0 & -1 & 0 & 0 & 2 & -1 \\ 0 & 0 & 0 & 0 & 0 & 0 & 0 & 0 & 0 & 0 & 0 & 1 & 0 & -1 & 2 \end{bmatrix}$$

$$|H| = L - L^{-1} = \begin{bmatrix} 2 & 1 & 0 & 1 & 0 & 0 & 0 & 0 & 0 & 0 & 0 & 0 & 0 & 0 & 0 \\ 1 & 4 & 1 & 0 & 1 & 0 & 1 & 0 & 0 & 0 & 0 & 0 & 0 & 0 & 0 \\ 0 & 1 & 2 & 1 & 0 & 0 & 0 & 0 & 0 & 0 & 0 & 0 & 0 & 0 & 0 \\ 1 & 0 & 1 & 2 & 0 & 0 & 0 & 0 & 0 & 0 & 0 & 0 & 0 & 0 & 0 \\ 0 & 1 & 0 & 0 & 2 & 1 & 0 & 0 & 0 & 0 & 0 & 0 & 0 & 0 & 0 \\ 0 & 0 & 0 & 0 & 1 & 2 & 1 & 0 & 0 & 0 & 0 & 0 & 0 & 0 & 0 \\ 0 & 1 & 0 & 0 & 0 & 1 & 2 & 0 & 0 & 0 & 0 & 0 & 0 & 0 & 0 \\ 0 & 0 & 0 & 0 & 0 & 0 & 0 & 2 & 1 & 0 & 0 & 0 & 1 & 0 & 0 \\ 0 & 0 & 0 & 0 & 0 & 0 & 0 & 1 & 2 & 1 & 1 & 1 & 0 & 0 & 0 \\ 0 & 0 & 0 & 0 & 0 & 0 & 0 & 0 & 1 & 2 & 1 & 1 & 0 & 0 & 1 \\ 0 & 0 & 0 & 0 & 0 & 0 & 0 & 0 & 1 & 1 & 2 & 1 & 1 & 0 & 0 \\ 0 & 0 & 0 & 0 & 0 & 0 & 0 & 0 & 1 & 1 & 1 & 2 & 0 & 1 & 0 \\ 0 & 0 & 0 & 0 & 0 & 0 & 0 & 1 & 0 & 0 & 1 & 0 & 2 & 0 & 0 \\ 0 & 0 & 0 & 0 & 0 & 0 & 0 & 0 & 0 & 0 & 0 & 1 & 0 & 2 & 1 \\ 0 & 0 & 0 & 0 & 0 & 0 & 0 & 0 & 0 & 1 & 0 & 0 & 0 & 1 & 2 \end{bmatrix}$$

2.16. There are more relations if $|H|$ is similar to H [17]. In particular, the eigenvalues 0 of H which belong to the harmonic 1-forms lead to eigenvalues -1 of L and the eigenvalues 0 of H which belong to harmonic 0-forms lead to eigenvalues 1 of L [17].

2.17. The relation could also be useful to analyze the distribution of the Laplacian eigenvalues, especially in the upper part of the spectrum. We can apply the Schur inequality for L to get

$$\sum_{i=1}^t \lambda_i \leq t$$

for the ordered list of eigenvalues λ_i of L . As eigenvalues of L are first negative this is a suboptimal lower bound for small t . But as there is an equality for $t = n$, there will be a compensation in the upper part. This gives lower bounds on the largest eigenvalues of L . By the way, also the Fiedler inequality giving the lower bound of $d \leq \delta(H) \leq 2d$ follows directly from Schur. But for L Schur gives have $n - 1 \leq \delta(L) \leq n$.

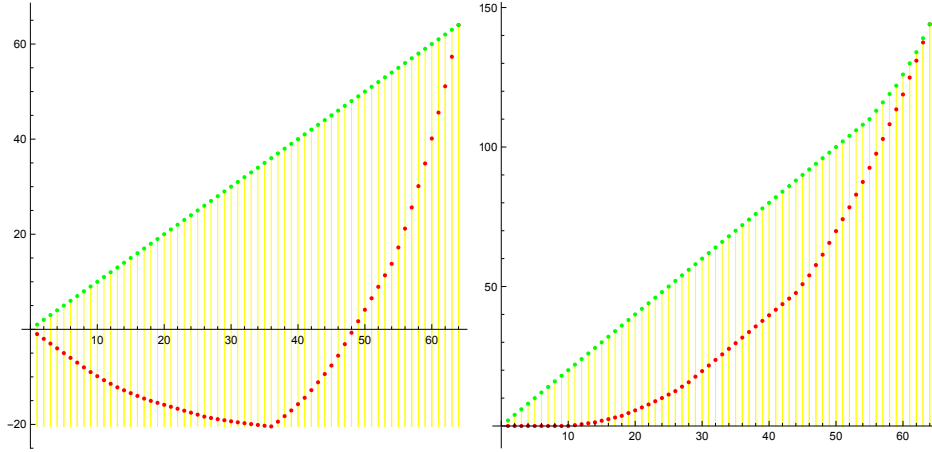


FIGURE 2. An illustration of the Schur inequality first for L and then for $|H| = L - L^{-1}$. The inequality allows for example to estimate the gap between the largest λ_n and second largest eigenvalue λ_{n-1} . The simplest estimate is $\lambda_n(L) - \lambda_{n-1}(L) \geq 1$. For $|H|$, Schur gives the Fiedler inequality $\lambda_n(|H|) \geq d$, where d is the largest vertex degree. Better estimates can be obtained by taking powers L^k . One can estimate the largest gap $\lambda_n(L) - \lambda_{n-1}(L) \geq P(k)^{1/k}$ from the maximal number $P(k)$ of closed paths of length k in G' .

2.18. Here is quadratic relation which illustrates the relation with a random walk: we know $\|\lambda\|_2^2 = \sum_{i=1} \lambda_i^2 = \sum_{i,j} L_{ij}^2 = \text{tr}(L^2) = \sum_{i,j} L_{ij}$ to hold for any simplicial complex G . In the 1-dimensional case, the eigenvalues of L^2 are the eigenvalues of L^{-2} so that the eigenvalues λ of L satisfy $\|\lambda\|_2^2 = \|\lambda^{-1}\|_2^2 = \text{tr}(L^{-2})$. So,

$$\text{tr}(|H|^2) = \text{tr}((L - L^{-1})^2) = 2\text{tr}(L^2) - 2n = 2\|\lambda\|_2^2 - 2n .$$

As $|H| = |H_0| \oplus |H_1|$ and $|H_0| = |d_0| * |d_0|$, $H_1 = |d_0| |d_0|^*$ are essentially isospectral, the left hand side is

$$2\text{tr}(|H_1|^2) = \sum_x \text{deg}'(x) = 4|E'| ,$$

where $\text{deg}'(x)$ is the vertex degree of the connection graph of G and $|E'|$ is the number of edges in the connection graph G' . As in the 1-dimensional case, the Euler characteristic satisfies $\chi(G) = \chi(G')$ as G' is homotopic to G (note that G' has triangles and is no more 1-dimensional), the energy theorem tells $\chi(G) = \sum_{i,j} L_{i,j}^{-1}$.

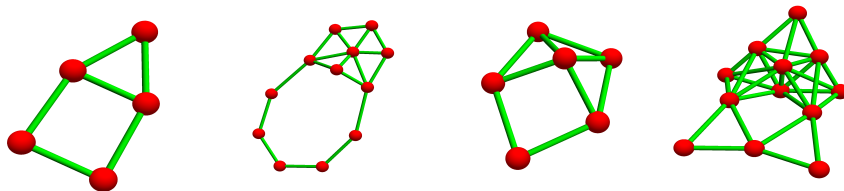


FIGURE 3. We see the house graph G , its Barycentric refinement G_1 , the line graph G_L and the connection graph G' . Both G_L and G_1 are subgraphs of G' . The hydrogen formula relates in full generality for any G the growth of the random walk in the line graph G_L with the growth of the random walk in the connection graph G' .

3. RANDOM WALKS

3.1. Squaring the hydrogen relations $L - L^{-1} = |H|$ gives $L^2 - 2 + L^{-2} = |H|^2$. We see that the sequence of vectors $\psi(n) = L^n \psi$ indexed by $n \in \mathbb{Z}$ satisfy the in both space and time discrete Laplace recursion relation

$$\Delta \psi = |H|^2 \psi,$$

where $\Delta u(n) = u(n+2) - 2u(n) + u(n-2)$ is a discrete Laplacian. It is really interesting that we get here a **two sided random walk** $\psi(n)$. This defines a scattering problem as we can look both at the asymptotic of $\psi(n)$ for $n \rightarrow +\infty$ and $n \rightarrow -\infty$. The limit $n \rightarrow \infty$ is well understood as L is a non-negative matrix which is irreducible. The vectors $\psi(n)/r^n$ converge to the Perron-Frobenius eigenvector, where r is the spectral radius. However $\psi(-n)/r^n$ behaves differently as the eigenfunction is different.

3.2. There is some affinity with a transfer matrix A for 1-dimensional Schrödinger equation $u(n+1) - u(n) + u(n-1) = V(n)u(n)$, where $V(n)$ is a $m \times m$ matrix. The model is there also known as a discrete Schrödinger operator on the strip and used to capture features of a two-dimensional discrete operator using methods from one dimensions. There, the $2m \times 2m$ matrix A is symplectic (meaning $A^T J A = J$ with the standard symplectic matrix J satisfying $J^2 = -1$ and $J^T = -J$). The matrix L^2 however is not symplectic in general as its size is not necessarily even. While any symplectic matrix S has a block structure

$$S = \begin{bmatrix} A & B \\ C & D \end{bmatrix}, S^{-1} = \begin{bmatrix} D^T & -B^T \\ -C^T & A^T \end{bmatrix},$$

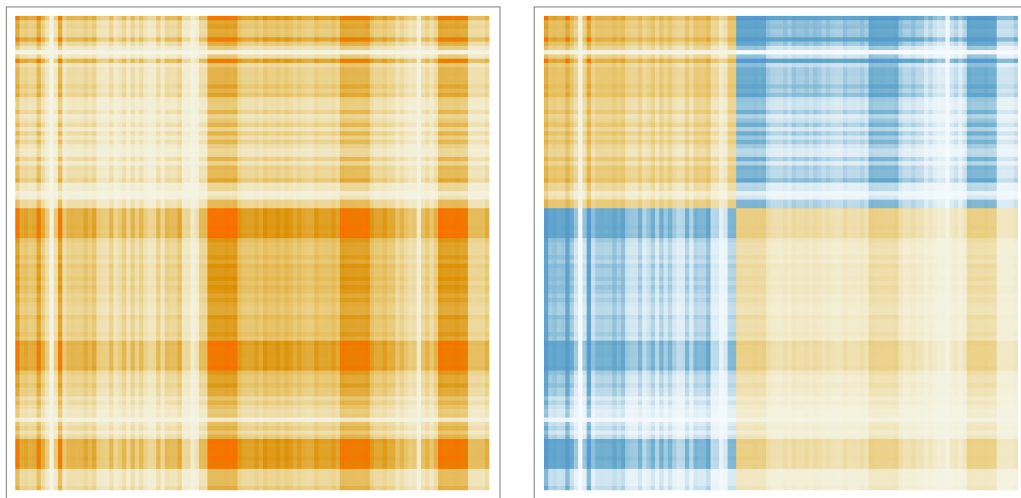


FIGURE 4. The matrix L^{2n}/ρ^{2n} converges to P , the projection of the Perron-Frobenius operator $v \otimes v$, where v is the eigenvectors of the largest eigenvalue $\rho(L)$ of L . Going backwards, the matrix L^{-2n}/ρ^{2n} however converges onto the projection $w \otimes w$, where w is the eigenvector of $1/\rho$ of L . Unlike the Perron-Frobenius operator v which is in the positive quadrant, the eigenvector w takes different signs.

the connection Laplacian L in the circular case satisfies

$$L = \begin{bmatrix} A & B \\ C & D \end{bmatrix}, L^{-1} = \begin{bmatrix} -D & B \\ C & -A \end{bmatrix}.$$

Still, in general, for 1-dimensional complexes, we have the spectral symmetry $\sigma(L^2) = \sigma(L^{-2})$ [16] which is shared by symplectic matrices. This motivates to investigate whether L^2 is conjugated to a symplectic matrix.

3.3. A symplectic matrix always has an even size and determinant 1. It has enjoys the spectral symmetry $\lambda \leftrightarrow 1/\lambda$, we know to happen for L^2 . The connection Laplacian L has determinant $-1, 1$. If the size of L is even, then L^2 has a chance to be symplectic because L^2 always has determinant 1 and the evenness obstacle is removed. Indeed:

Proposition 1 (Symplectic Kirby connection). *If G is a graph with n vertices and m edges and $n + m$ is even, then L^2 is similar to a symplectic matrix.*

Proof. The spectral symmetry implies that the characteristic polynomial of L^2 is reciprocal. A theorem of David Kirby (see Theorem A.1 in [26]) implies that the square L^2 of L is similar to a symplectic matrix. \square

3.4. The space of solutions of the 1-dimensional Jacobi equation

$$\Delta\psi(n) = |H|^2\psi(n)$$

with $\Delta u(n) = u(n+2) - 2u(n) + u(n-2)$ is $4n$ -dimensional because we have a second order recursion and two independent lattices. Because the sign-less Hodge operator $|H|$ has non-negative spectrum, it is not so much a “discrete wave equation” as a “discrete Laplace equation”. It shows the growth for $|n| \rightarrow \infty$ as harmonic functions do. As the wave equation needs an initial velocity and initial position and the Laplacian Δ has a smallest unit translation 2, it is natural to invoke quaternions:

Lemma 1 (Quaternion initial value). *The discrete Laplace equation $\Delta\psi(n, x) = |H|^2\psi(n, x)$ has a unique solution which is determined by a quaternion valued initial field $x \rightarrow \psi(0, x) \in \mathbb{H}$.*

Proof. Given a quaternion-valued function $\psi(x) = \psi_0(x) + i\psi_1(x) + j\psi_2(x) + k\psi_3(x)$ on the simplicial complex, we can span the solution space of the (4th order) Jacobi equation with

$$L^{2n}\psi_0, L^{-2n}\psi_1, L^{2n+1}\psi_2, L^{-2n-1}\psi_3 .$$

Both vector spaces are $4n$ -dimensional if $n = e + f$ is the number of simplices in the 1-dimensional simplicial complex defined by G . \square

4. REMARKS

4.1. It should be noted that the hydrogen relation $L - L^{-1} = |H|$ holds also over other fields F rather than the familiar real numbers. We can for example look at the relation over the finite field $F = \mathbb{Z}_p$ with a prime p . Because the matrices L and L^{-1} are integer-valued, we just can look at all the numbers modulo p . Now, the random walk $L^n\psi$ is a cellular automaton in the sense of Hedlund [9]. The alphabet is the set of F -valued functions from the simplicial complex G to F . As a random walk, the state $L^n\psi$ is a path integral, summing over all paths of length n in the graph G' in which some self loops are attached to each node.

Proposition 2 (Reversible cellular automaton). *The hydrogen relation $|H| = L - L^{-1}$ still holds over finite fields F . The corresponding random walk $L^n\psi$ is a reversible cellular automaton over a finite alphabet F^G .*

A cellular automaton defines a homeomorphism T on the compact metric space $\Omega = A^{\mathbb{Z}}$, where $A = F^G$ is the finite alphabet of all F valued functions on G . The dynamics T commutes with the shift. This is the point of view of Hedlund [9]. By the theorem of Curtis-Hedlund and Lyndon, the shift commuting property is equivalent to the existence of a finite rule involving only a finite neighborhood. In the theory of cellular automata, one looks at the attractor $\bigcap T^k \Omega$ which defines a subshift of finite type. Of interest is the structure of invariant measures or whether the automaton is prime. (See i.e. [10] which sees cellular automata in the eyes of Hedlund.)

4.2. In the Barycentric limit, both the spectral measure of L and the spectral measure of H converge. In one dimension, the limiting operator of H is given by a Jacobi matrix while L is a Jacobi matrix on a strip. It still has the property $L - L^{-1} = |H|$. Because already after one Barycentric refinement, we have a bipartite graph, the sign-less Laplacian $|H|$ is similar to H . The limiting density of states of both L and H are known. The limiting spectral function for H is $F(x) = 4 \sin^2(\pi x/2)$. It satisfies $F(2x) = T(F(x))$ with $T(x) = x(4 - x)$. In the finite dimensional case, the spectral function is defined as $F_n(x) = \lambda_{[nx]}$, where $[nx]$ is the floor function and the eigenvalues are $\lambda_0, \dots, \lambda_{n-1}$. Since the eigenvalues μ_k of L satisfy $\phi(\mu_k) = \mu_k - 1/\mu_k = \lambda_k$, the spectral function of L is the pull-back under ϕ .

Proposition 3. *The hydrogen relation $|H| = L - L^{-1}$ holds also in the Barycentric limit. The operator L as well as its inverse L^{-1} both remain bounded.*

We have made use of this already when looking at the limiting Zeta function for L [16].

4.3. For 1-dimensional Schrödinger operators [23, 24, 3], given in the form of general Jacobi matrices $Hu(n) = a(n)u(n+1) + a(n-1)u(n-1) + b(n)u(n)$, one has hopping terms $a(n)$ attached to directed edges, and terms $b(n)$ attached to self-loops. Adjacency matrices of weighted graphs or Laplacians (which have row summing up to zero) are also called “discrete elliptic differential operators” [5] and the zero sum case is a “harmonic Laplacian”. The circular graph case has also a “covering version” where one looks at the Floquet theory of periodic operators or more generally at almost periodic or random cases like “almost Mathieu” $a(n) = 1, b(n) = c \cos(\theta + n\alpha)$, where $a(n) = f(T^n x), b(n) = g(T^n x)$ are defined by translations on a compact topological group. The flat Laplacian $Hu(n) = u(n+1) - 2u(n) + u(n-1)$ on \mathbb{Z} is a bounded operator on $l^2(\mathbb{Z})$ has the spectrum on $[0, 4]$. We

usually don't think about this operator as an almost periodic operator, but its nature is almost periodic if we look at it as a Barycentric refinement limit, where the hydrogen relation $|H| = L - L^{-1}$ still works. In order to see the Jacobi structure in the cyclic case, we have to order the complex as $Z = \{\dots \{-1, 0\}, \{0\}, \{0, 1\}, \{1\}, \{1, 2\} \dots\}$ as seen in Figure (5). The hydrogen relation $|H| = L - L^{-1}$ still holds and L is a Jacobi matrix "on the strip". With that ordering we have $|H|u(n) = u(n+2) + 2u(n) + u(n-2)$, which is isospectral to $Hu(n) = -u(n+2) + 2u(n) - u(n-2)$.

4.4. For any 1-dimensional complex G with n simplices and any discrete Laplacian H close to the standard Hodge Laplacian $|H|$ satisfying $H(x, y) = 0$ if $x \cap y = \emptyset$, there is a connection operator L such that $H = L - L^{-1}$ holds. In that case, both L and L^{-1} have zero entries $L(x, y) = L^{-1}(x, y)$ if x, y do not intersect. We just need to compute the determinant of the derivative $d\phi$ of the map $\phi : L \rightarrow \pi(L - L^{-1})$ on the finite dimensional space $X = \{A \in M_n(\mathbb{R}) \mid A = A^T, A(x, y) = 0 \text{ if } x \cap y = \emptyset.\}$. Here π is the projection onto X . Given an operator $H \in X$. We want to write it as $H = L - L^{-1}$. One can construct L near a known solution by apply the Newton step to the equation $\phi(L) = H - L + L^{-1} = 0$ in order to solve the $H_{ij} - L_{ij} + g_{ij}(L) = 0$, which are rational functions in the unknown entries L_{ij} as $g = L^{-1}$ has explicit Cramer type rational expressions.

4.5. An important open question is how to extend the hydrogen relation to higher dimensional complexes. We would like to write the sign-less Hodge operator $|H|$ as a sum $L - L^{-1}$ where L has the spectral symmetry that L^2 and L^{-2} have the same spectrum. If such a symmetric extension is not possible, we can still look at the relation $L - L^{-1} = K$ anyway. It is just that K is not a Hodge Laplacian any more. In higher dimensions, the spectrum of H can have negative parts. Still, we can interpret the solution $L^n \psi$ of the reversible random walk as a solution of the Laplace equation $\Delta \psi = K^2 \psi$.

4.6. Next, we look at the question about the robustness of the hydrogen relation. Can it be extended to situations in which the interaction between simplices is not just $L(x, y) = 1$ but a number $1 + \epsilon(x, y)$? The answer is yes, (in some rare cases like the circular a conservation law has to be obeyed as otherwise, the symmetry produces a zero Jacobean determinant not allowing the implicit function theorem to be applied. It is quite remarkable that $|H| = L - L^{-1}$ for finite range Laplacians H, L can be perturbed so that in the perturbation, still both L and H are finite range implying that L^{-1} has finite range. The simplest case

is the Jacobi case, where the graph is a linear graph or circular graph. The hydrogen relation might go over to perturbations in the infinite dimensional case as we have a Banach space of bounded operators. A technical difficulty is to verify that the Jacobean operator of the map $L \rightarrow L - L^{-1}$ is bounded and invertible.

4.7. For random Jacobi matrices, where $a(n), b(n)$ are defined by a dynamical system T , the relation $L - L^{-1} = H$ requires that T is renormalized in the sense that it is an integral extension of an other system. (The word “random operator” is here used in the same way than “random variable” in probability theory; there is no independence nor decorrelation assumed.) Let us restrict to \mathbb{Z} , so that time is 1-dimensional and where the $a(n), b(n)$ can be given by an integral extension S of an automorphism T of a probability space or an integral extension S of a homeomorphism T of a compact metric space. (An integral extension of $S : X \rightarrow X$ is $T((x, 1)) = (x, 2)$ and $T((x, 2)) = (Sx, 1)$. It satisfies $S^2 = T$ so that S^2 is never ergodic. Not all dynamical systems are integral extensions; mixing systems are never integral extensions.)

4.8. We believe that for any random Jacobi matrix $Hu(n) = a(n)u(n+2) + a(n-2)u(n-2) + b(n)u(n)$ close enough to $a = 0, b = 2$, there is a Jacobi matrix $Lu(n) = c(n)u(n+2) + d(n)u(n+1) + c(n-2)u(n-2) + d(n-1)u(n-1) + e(n)u(n)$ of the same type for which the hydrogen relation $H = L - L^{-1}$ holds. The condition of being a Jacobi matrix of this type can be rephrased as an equation $G(L, H) = 0$ by bundling all conditions $[H - L + L^{-1}]_{i,j} = 0$ for all i, j and $L_{i,j} = 0$ for all $|i - j| > 2$. If $\partial_L G(L, H)$ is invertible, it is possible to compute the functional derivative of $\psi_{ij}(L) = [H - L + L^{-1}]_{ij}$ and assure that the inverse L^{-1} is a Jacobi matrix in a strip. The hydrogen relation $H = L - L^{-1}$ gives then that L^{-1} is a Greens function of the same finite range. A priori, it only is a Toeplitz operator and not a Jacobi matrix. It would of course be nicer to have explicit formulas for L , similarly as we can compute D satisfying $L = D^2 + E$ for E in the resolvent set of L in terms of Titchmarsh-Weyl m -functions.

4.9. Simplicial complexes define a ring. The addition in this “strong ring” is obtained by taking the disjoint union. This monoid can be extended with the Grothendieck construction (in the same way as integers are formed from the additive monoid of natural numbers or fractions are formed from the multiplicative monoid of non-zero integers) to a group in which the empty complex 0 is the zero element. The Cartesian product of two complexes is not a simplicial complex any more. One

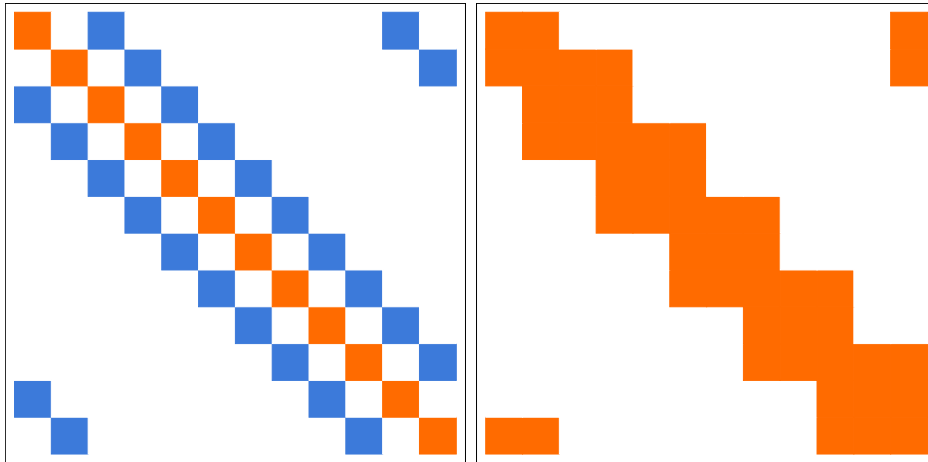


FIGURE 5. The Hodge operator H of the Laplacian H_0 on the circular graph is seen here with the ordering so that H is again a Laplacian, but on a larger scale (this is the trivial renormalization picture) and the connection Laplacian L . We display here periodic matrices but in the limit we have operators on $l^2(\mathbb{Z})$ the hydrogen relation $|H| = L - L^{-1}$ still holds. The matrix L can not be diagonalized with Fourier. We needed the hydrogen relation to diagonalize L [16].

can however look at the ring generated by simplicial complexes. This ring is a unique factorization domain and the simplicial complexes are the primes [15]. We call it the strong ring because the corresponding connection graphs multiply with the strong product in graph theory. One can now define both a connection matrix $L(A \times B)$ as well as a Hodge operator $H(A \times B)$. If A has n elements and B has m elements, then $L(A \times B)$ and $H(A \times B)$ are both $nm \times nm$ matrices. If λ_k are the eigenvalues of $L(A)$ and μ_k are the eigenvalues of $L(B)$, then $\lambda_k \mu_l$ are the eigenvalues of $L(A \times B)$. If λ_k are the eigenvalues of $H(A)$ and μ_k are the eigenvalues of $H(B)$ then $\lambda_k + \mu_l$ are the eigenvalues of $H(A \times B)$. We can now ask whether the product operators $L(A \times B)$ and $H(A \times B)$ still satisfy the hydrogen relations. This is not true, but also not to be expected. What still happens in general for all simplicial complexes that $g = L(A \times B)^{-1}$ satisfies the energy theorem $\sum_{x \in A \times B} \sum_{y \in A \times B} g(x, y) = \chi(A \times B) = \chi(A)\chi(B)$. Also, in the 1-dimensional case, still $L^2(A \times B)$ has the same spectrum than $L^{-2}(A \times B)$.

4.10. If we think of $L - L^{-1}$ as a 1-dimensional derivative and $L^2 - 2 + L^{-2}$ as a second derivative, then we can look at $\Delta = L_A^2 - 2 + L_A^{-2} + L_B^2 - 2 + L_B^{-2}$ as a discrete Laplacian leading to a random walk $\Delta u = L^2(A \times B)u$ parametrized by a two dimensional time. Again, given a quaternion valued function on the simplices of the graph gives now a unique solution $u(n, m) = L_A^n L_B^m u$. This can be generalized to any dimension. In this model, we should think of the graph G as the “fibre” over a discrete lattice. An other way to think about it is to see the lattice Z^2 as a two-dimensional time for a stochastic process on the graph. The stochastic process is interesting because it describes a classical random walk in a graph if time is positive. That this random walk can be reversed allows to walk backwards, again with finite propagation speed. While the backwards process given by L_A^{-1} or L_B^{-1} is still propagating in the same way than the forward random walk, it is not Perron-Frobenius. There is an arrow of time.

4.11. What is interesting about the hydrogen formula $L - L^{-1} = |H|$ is that the scales are fixed. If we insist L to be integer valued, we can not wiggle any coefficients, nor multiply H with a factor. In comparison, in [12] we have for numerical purposes time discretized a Schrödinger equation $ihu' = Lu$ with bounded Hamiltonian L by scaling the constant such that L has a small norm. We then looked at a discrete time dynamics for a deformed operator which interpolates the continuum differential equation. While the deformation does change the spectrum it does not the nature of the spectral measures (like for example whether it is singular continuous, absolutely continuous or pure point), the method is especially useful, using the Wiener criterion, to measure numerically whether some discrete spectrum is present. The analogy is close: we had defined $U = L \pm i\sqrt{1 - L^2}$ so that $U + 1/U = 2L$. If $\psi(t) = \exp(itL/h)$ is the quantum evolution, then $\psi(n + 1) + \psi(n - 1) = 2L\psi(n)$ with $\psi(n) = U^n\psi$. Now $U^n = \exp(inL) = \cos(in \arccos(L)) + i \sin(in \arccos(L)) = T_n(L) + iR_n(L)$ which are Tchebychev polynomials of L . This can be done faster than matrix exponentiation and leads to finite propagation speed, a property which $\exp(itL/h)$ does not enjoy. For numerical purposes, it allowed to make sure that no boundary effects play a role or that the process can be run using exact rational expressions. We have used the method to measure the spectrum of almost periodic operators like the almost Mathieu operator, where the spectrum is understood or magnetic two-dimensional operators, where the spectrum is not understood. In the present hydrogen relation, we can not scale L . In some sense, the Planck constant is fixed.

4.12. It could be interesting to look at the frame work in the context of a random geometric model called “Causal Dynamical Triangulations” [11]. This is a situation where a sequence G_k of 1-dimensional simplicial complexes is given by some time evolution. For the following it is not relevant how G_k are chosen as long as they are given by a dynamical process and the number of simplices is fixed. If L_k are the connection Laplacians of G_k , we can look at the system $L_{k+1} - L_{k-1}^{-1} = V_k$. The random walk becomes a cocycle $\psi_k = L_k \cdots L_2 L_1 \psi$ and the spectral radius ρ becomes a Lyapunov exponent.

4.13. If the sequence of graphs with the same number of vertices and edges, the orbit closure defines an ergodic random process. By Oseledec’s theorem, the Lyapunov exponent exists. Mathematically, the problem $u(n+2) - 2u(n) + u(n-2) = V_n u(n)$ is now a ergodic Jacobi operator on the strip, in which the graphs G_k are the fibers. The condition that the total number of vertices and edges remain constant is a topological condition. We could also insist that G_k have all the same topology. The solution space is then described by a quaternion-valued field: the hydrogen relations are already second order and we have an even and odd branch of time \mathbb{Z} which evolve independently. So there are four wave function components needed to determine the initial condition.

4.14. The ergodic situation is interesting because in a random setup, there is a chance to get localization and so obtain solutions $\psi(n) = L^n \psi$ which go to zero both for $n \rightarrow \infty$ as well as $n \rightarrow -\infty$. A concrete question is to construct a finite set of graphs $\{G_1, \dots, G_k\}$ with corresponding connection Laplacians $\{L_1, \dots, L_k\}$ so that for almost all two sided sequences $\omega \in \{1, 2, \dots, k\}^{\mathbb{Z}}$ there exists $\psi_\omega(0)$ such that the random walk in a random environment

$$(1) \quad \psi_\omega(n) = L_{\omega(n)} L_{\omega(n-1)} \cdots L_{\omega(2)} L_{\omega(1)} \psi(0)$$

has the property that $|\psi_\omega(n)| \rightarrow 0$ for $|n| \rightarrow \infty$. This does not look strange if comparing with the Anderson localization picture, where symplectic transfer matrices lead by Oseledec to almost certain exponential growth in one direction, but where it is possible that for almost all ω in the probability space, one has a complete set of eigenfunctions (which decay both forward and backward in time). In our case now, it is all just random walks $\psi(n)$ on a dynamically changing graphs.

4.15. The dynamical triangulation picture suggests to start with a single abstract simplicial complex G and think of G as a “space time manifold” with the property G is a disjoint union of finite abstract

simplicial complexes $G = \{G_k\}_{k \in \mathbb{Z}}$ for which each G_k has the same cardinality m . We don't really need to assume the "time slices" G_k to be 1-dimensional. Each G_k has a connection Laplacian L_k . Because there are only a finite set A of simplicial complexes with m simplices, the space-time complex G defines an element in the compact metric space $A^{\mathbb{Z}}$. As usual in symbolic dynamics, the single sequence G defines its orbit closure Ω (the subset of all accumulation points which is a shift-invariant and closed subset). A natural assumption (avoiding many-world interpretations), is that the shift is uniquely ergodic; the complex G alone determines a unique natural probability space (Ω, μ) .

4.16. One can now study the properties of the random walk $\psi_\omega(n)$ given in (1). The unimodularity theorem assures that L_k are invertible and in the 1-dimensional case (if m is even) also symplectic. The structure of the inverse $g = L^{-1}$ assures that the random walk is two sided and that also the inverse is a random walk as the transition steps $g(x, y) = L^{-1}(x, y)$ are defined by the Green star formula [17]. The Anderson localization picture suggests the existence of examples, where $\|\psi_\omega(n)\|_2$ is bounded. The $\psi(n)$ are solutions to a reversible random walk, but they are also localized. They solve $\Delta\psi = K\psi$ with $K = (L - L^{-1})^2$ which is a Wheeler-DeWitt type eigenvalue equation. It describes the reversible random walk in a random environment so that solutions are path integrals. The model is robust in the sense that if we perturb $K = H^2$, we can still write $L - L^{-1} = H$ with operators L, L^{-1} which have the same support and so finite propagation speed.

5. MATHEMATICA CODE

5.1. We construct a random graph, compute both L and $|H|$ then check the hydrogen relation $L - L^{-1} - |H| = 0$.

```
(* The sign-less Hydrogen relation, O. Knill, 2/10/2018 *)
{v,e}={30,80}; s=RandomGraph[{v,e}]; n=v+e;
bracket[x_]:= {x}; set[x_]:= {x[[1]],x[[2]]};
G=Union[Map[set,EdgeList[s]],Map[bracket,VertexList[s]]];
m[a_,b_]:= If[SubsetQ[a,b]&&(Length[a]==Length[b]+1),1,0];
d=Table[m[G[[i]],G[[j]]],{i,n},{j,n}]; (* signl. deriv *)
Dirac=d+Transpose[d]; H=Dirac.Dirac; (* signl. Hodge *)
L=Table[If[DisjointQ[G[[k]],G[[1]]],0,1],{k,n},{1,n}];
Total[Flatten[Abs[(L-Inverse[L]) - H]]]
```

The various spectral radius estimates can be compared. In the various tables, we first compute $\rho = \rho(H)$, then $|\rho| = \rho(|H|)$, then $r - 1/r$ with $r = 1 + (\max_x P(3, x))^{1/3}$, then $r - 1/r$ with $r = 1 + \max_{x,y \in E} d(x) + d(y)$, then the edge estimates and vertex degree estimates which involve the diameter of the graph.

```
(* Estimating the spectral radius, O. Knill, 2/18/2018 *)
ClearAll["Global`*"];
L[s_]:=Module[{v=VertexList[s],e=EdgeList[s],n,G,L},b[x_]:= {x};
p[x_]:= {x[[1]],x[[2]]};G=Union[Map[p,e],Map[b,v]];n=Length[G];
Table[If[DisjointQ[G[[k]],G[[1]]],0,1],{k,n},{1,n}]];
Barycent[s_]:=Module[{v=VertexList[s],e=EdgeList[s],V,W},
p[x_]:= {x[[1]],x[[2]]}; W=Flatten[Table[
{p[e[[k]]]->e[[k,1]],p[e[[k]]]->e[[k,2]]},{k,Length[e]}]];
V=Union[v,Map[p,e]];UndirectedGraph[Graph[V,W]];BC=Barycent;
sprime[s_]:=AdjacencyGraph[L[s]-IdentityMatrix[Length[L[s]]]];
Rho[s_]:=Max[Eigenvalues[1.0 Normal[KirchhoffMatrix[s]]]];
Rhoa[s_]:=Max[Eigenvalues[1.0 Abs[Normal[KirchhoffMatrix[s]]]]];
Walk[s_,k_]:=Max[Map[Total,MatrixPower[AdjacencyMatrix[s],k]]];
VD=VertexDegree; (* next comes Shi and Li-Shiu-Chang estimates*)
ShLiShCh[s_]:=Module[{R=GraphDiameter[s],g=VD[s],d,v},
d=Max[g];v=Length[VertexList[s]];N[2d-1/(v(2R+1))]];
StBrHo[s_]:=Module[{e,sp=sprime[s]},(* Stanley-Brualdi-Hoffmann*)
e=Length[EdgeList[sp]];u=1+N[(Sqrt[1+8e]-1)/2];u-1/u];
Deg2[s_]:=Module[{e=EdgeList[s],v=VertexList[s],r},
d[k_]:=1+VD[s,v[[e[[k,1]]]]+VD[s,v[[e[[k,2]]]]];
r=Max[Table[d[k],{k,Length[e]}]];N[r-1/r]];
Walk3[s_]:=Module[{r=1+(Walk[sprime[s],3])^(1/3)},N[r-1/r]];
F[s_]:= {Rho[s],Rhoa[s],Walk3[s],Deg2[s],StBrHo[s],ShLiShCh[s]};
Table[F[CompleteGraph[{3,k}]],{k,3,9}] // MatrixForm
Table[F[CycleGraph[k]],{k,4,10}] // MatrixForm
Table[F[CompleteGraph[k]],{k,2,8}] // MatrixForm
Table[F[StarGraph[k]],{k,4,10}] // MatrixForm
Table[F[WheelGraph[k]],{k,5,11}] // MatrixForm
Table[F[PetersenGraph[6,k]],{k,2,8}] // MatrixForm
Table[F[GridGraph[{k,1}]],{k,2,8}] // MatrixForm
Table[F[GridGraph[{6,k}]],{k,2,8}] // MatrixForm
Table[F[RandomGraph[{20,5}]],{7}] // MatrixForm
Table[F[RandomGraph[{20,50}]],{7}] // MatrixForm
Table[F[RandomGraph[{30,100}]],{7}] // MatrixForm
Table[F[BC[RandomGraph[{20,100}]],{7}]] // MatrixForm
```

6. MEASUREMENTS

6.1. The following tables were obtained by running the code displayed in the above section. In each case, we see the spectral radius ρ , the sign-less spectral radius $|\rho|$, the dual vertex estimate, a three step walk estimate, then a global edge estimate and finally an upper bound obtained in [20].

6.2. Complete bipartite Graphs are computed from $K_{3,3}$ (utility graph) to $K_{3,9}$. These are regular graphs for which [20] do not apply. Indeed, we see that the estimate is then below the actual spectral radius

ρ .

ρ	$ \rho $	Thm (2)	3Walk	[2, 28]	[20]
6.	6.	6.85714	6.22655	8.88889	5.96667
7.	7.	7.875	7.23871	10.8126	7.97143
8.	8.	8.88889	8.24856	12.6793	9.975
9.	9.	9.9	9.25665	14.5115	11.9778
10.	10.	10.9091	10.2634	16.3213	13.98
11.	11.	11.9167	11.269	18.1156	15.9818
12.	12.	12.9231	12.2739	19.8985	17.9833

6.3. Cyclic graphs are computed from C_4 to C_{10} . Also these are regular graphs.

ρ	$ \rho $	Thm (2)	3Walk	[2, 28]	[20]
4.	4.	4.8	4.19371	5.24008	3.95
3.61803	4.	4.8	4.19371	5.83333	3.96
4.	4.	4.8	4.19371	6.36744	3.97619
3.80194	4.	4.8	4.19371	6.85714	3.97959
4.	4.	4.8	4.19371	7.31193	3.98611
3.87939	4.	4.8	4.19371	7.73832	3.98765
4.	4.	4.8	4.19371	8.14105	3.99091

6.4. Complete Graphs are computed from K_2 (interval) to K_8 (an 7 dimensional simplex). These are regular graphs for which [20] do not apply.

ρ	$ \rho $	Thm (2)	3Walk	[2, 28]	[20]
2.	2.	2.66667	2.20091	2.17116	1.83333
3.	4.	4.8	4.19371	4.56245	3.88889
4.	6.	6.85714	6.22655	7.31193	5.91667
5.	8.	8.88889	8.24856	10.4174	7.93333
6.	10.	10.9091	10.2634	13.8539	9.94444
7.	12.	12.9231	12.2739	17.5971	11.9524
8.	14.	14.9333	14.2817	21.6258	13.9583

SPECTRAL RADIUS

6.5. Star Graphs are computed starting with central degree 3 to central degree 9.

ρ	$ \rho $	Thm (2)	3Walk	[2, 28]	[20]
4.	4.	4.8	4.19371	4.56245	5.95
5.	5.	5.83333	5.21154	5.64311	7.96
6.	6.	6.85714	6.22655	6.69818	9.96667
7.	7.	7.875	7.23871	7.73832	11.9714
8.	8.	8.88889	8.24856	8.76893	13.975
9.	9.	9.9	9.25665	9.79308	15.9778
10.	10.	10.9091	10.2634	10.8126	17.98

6.6. Wheel Graphs are computed with central degree 4 up to central degree 10

ρ	$ \rho $	Thm (2)	3Walk	[2, 28]	[20]
5.	6.56155	7.875	6.99565	8.64722	7.96
6.	7.23607	8.88889	7.8263	9.9	9.96667
7.	8.	9.9	8.69993	11.0994	11.9714
8.	8.82843	10.9091	9.60356	12.2617	13.975
9.	9.70156	11.9167	10.5285	13.3969	15.9778
10.	10.6056	12.9231	11.4687	14.5115	17.98
11.	11.5311	13.9286	12.4203	15.6102	19.9818

6.7. Peterson Graphs Peterson(6, k) are computed for $k = 2$ to $k = 8$.

ρ	$ \rho $	Thm (2)	3Walk	[2, 28]	[20]
5.23607	6.	6.85714	6.22655	12.4305	5.99074
5.41421	5.41421	6.85714	5.92748	10.8126	5.99074
5.23607	6.	6.85714	6.22655	12.4305	5.99074
6.	6.	6.85714	6.22655	12.4305	5.99074
5.23607	5.23607	6.85714	5.87411	10.8126	5.99242
6.	6.	6.85714	6.22655	12.4305	5.99074
5.23607	6.	6.85714	6.22655	12.4305	5.99074

6.8. Linear Graphs are taken from length 1 to 7

ρ	$ \rho $	Thm (2)	3Walk	[2, 28]	[20]
2.	2.	2.66667	2.20091	2.17116	1.83333
3.	3.	3.75	3.17771	3.43141	3.93333
3.41421	3.41421	4.8	3.78886	4.31043	3.96429
3.61803	3.61803	4.8	3.96987	5.02531	3.97778
3.73205	3.73205	4.8	4.13272	5.64311	3.98485
3.80194	3.80194	4.8	4.16348	6.19493	3.98901
3.84776	3.84776	4.8	4.19371	6.69818	3.99167

6.9. Grid graphs $G(6, k)$ with $k = 2$ to $k = 8$ lead to

ρ	$ \rho $	Thm (2)	3Walk	[2, 28]	[20]
5.73205	5.73205	6.85714	6.20288	11.3786	5.99359
6.73205	6.73205	8.88889	7.78401	15.4104	7.9963
7.14626	7.14626	8.88889	8.00389	18.564	7.99755
7.35008	7.35008	8.88889	8.211	21.2437	7.99825
7.4641	7.4641	8.88889	8.22357	23.6148	7.99868
7.53399	7.53399	8.88889	8.23608	25.7644	7.99896
7.57981	7.57981	8.88889	8.23608	27.7449	7.99917

6.10. Now, we take **random graphs** with 20 vertices and 4 edges:

ρ	$ \rho $	Thm (2)	3Walk	[2, 28]	[20]
5.08613	5.08613	6.85714	5.49603	6.19493	8.
3.	3.	3.75	3.17771	5.24008	4.
3.	3.	3.75	3.17771	5.02531	4.
3.	3.	3.75	3.17771	5.02531	4.
4.	4.	4.8	4.19371	5.44565	6.
4.	4.	4.8	4.19371	5.44565	6.
2.	2.	2.66667	2.20091	4.8	2.

6.11. Random graphs with 20 vertices and 50 edges:

ρ	$ \rho $	Thm (2)	3Walk	[2, 28]	[20]
10.5926	12.7038	17.9444	15.0334	26.5056	17.9944
9.28796	11.0103	13.9286	12.4608	25.4858	13.9929
11.3603	12.7573	17.9444	15.0837	26.7353	17.9944
10.8116	12.1925	17.9444	14.6776	26.1572	17.9929
10.6623	12.5725	17.9444	14.9725	26.2738	17.9944
10.447	12.8607	16.9412	14.9606	26.4671	18.
10.1163	11.308	15.9375	13.2007	25.6454	15.9929

6.12. Random graphs with 30 vertices and 100 edges:

ρ	$ \rho $	Thm (2)	3Walk	[2, 28]	[20]
14.4959	16.4624	23.9583	19.885	41.32	25.9963
13.2345	15.5212	20.9524	18.0239	41.2219	21.9963
12.7587	15.8331	20.9524	18.3655	41.5886	21.9963
12.255	14.7693	18.9474	16.6416	40.7278	19.9963
15.5824	16.9586	25.9615	20.944	41.7586	27.9952
13.0898	15.7372	20.9524	18.2323	41.4179	21.9963
13.6639	16.0848	22.9565	19.4197	41.1974	23.9963

6.13. Random graphs obtained by a Barycentric refinement of a random graph with 20 vertices and 100 edges:

SPECTRAL RADIUS

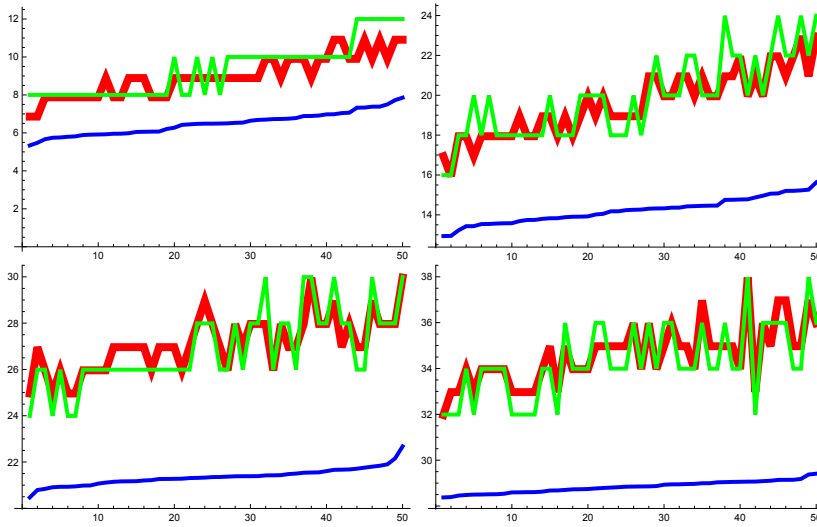


FIGURE 6. We see measurements with random graphs from $E(20, p)$ with $p = 0.1, 0.3, 0.5, 0.7$. 50 experiments were done in each case. The lowest curve is $\rho(G)$. The thin green is the estimate $2d-Q$, with Q small, estimated by many authors. The red (thicker) curve is the dual vertex degree estimate given in (2). It is more effective for small p .

ρ	$ \rho $	Thm (2)	3Walk	[2, 28]	[20]
15.099	15.099	16.9412	16.1703	54.2612	27.9994
14.2081	14.2081	15.9375	15.2196	53.9441	25.9994
15.0969	15.0969	16.9412	16.1299	54.0002	27.9994
15.1967	15.1967	16.9412	16.2192	54.798	27.9994
15.0951	15.0951	16.9412	16.1226	54.2984	27.9994
15.1091	15.1091	16.9412	16.1761	54.4654	27.9994
16.0813	16.0813	17.9444	17.0785	54.0189	29.9994

6.14. Here are some computations illustrated graphically.

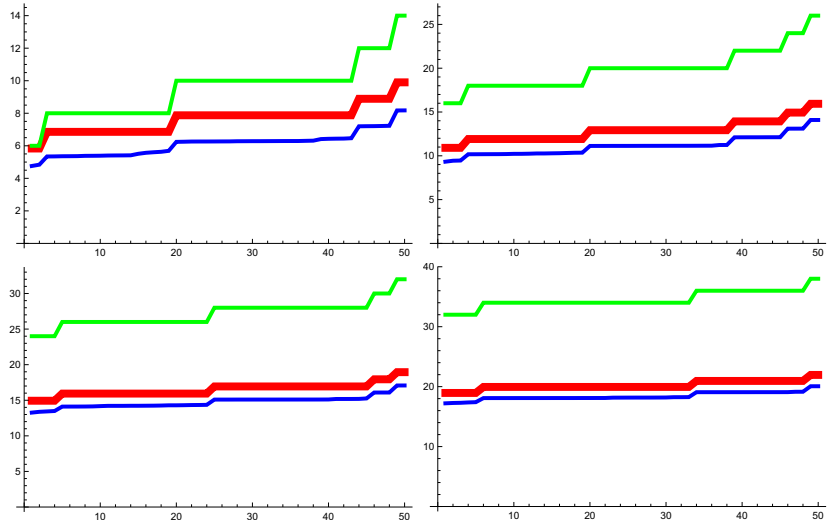


FIGURE 7. Measurements with random Barycentric refined graphs from $E(20, p)$ with $p = 0.1, 0.3, 0.5, 0.7$ are displayed. One can see again the estimate $2d - Q$ and then the dual vertex degree estimate.

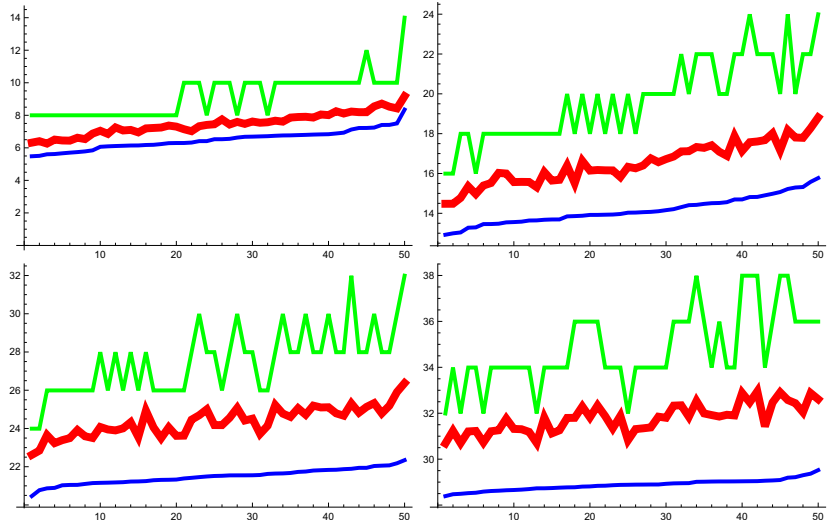


FIGURE 8. Measurements with random graphs from $E(20, p)$ are seen for $p = 0.1, 0.3, 0.5, 0.7$. The thick estimate is obtained by counting the number of walks of length 3 in the connection graph G' and taking the maximum. It is better than $2d - Q$ but it also uses a larger neighborhood of a vertex.

REFERENCES

- [1] W.N. Anderson and T.D. Morley. Eigenvalues of the Laplacian of a graph. *Linear and Multilinear Algebra*, 18(2):141–145, 1985.
- [2] R. A. Brualdi and A. J. Hoffmann. On the spectral radius of $(0,1)$ -matrices. *Linear Algebra and its Applications*, 65:133–146, 1985.
- [3] H.L. Cycon, R.G.Froese, W.Kirsch, and B.Simon. *Schrödinger Operators— with Application to Quantum Mechanics and Global Geometry*. Springer-Verlag, 1987.
- [4] K.Ch. Das. The Laplacian spectrum of a graph. *Comput. Math. Appl.*, 48(5-6):715–724, 2004.
- [5] Y.Colin de Verdière. *Spectres de Graphes*. Société Mathématique de France, 1998.
- [6] L. Feng, Q. Li, and X-D. Zhang. Some sharp upper bounds on the spectral radius of graphs. *Taiwanese J. Math.*, 11(4):989–997, 2007.
- [7] R. Grone and R. Merris. The Laplacian spectrum of a graph. II. *SIAM J. Discrete Math.*, 7(2):221–229, 1994.
- [8] Ji-Ming Guo. A new upper bound for the Laplacian spectral radius of graphs. *Linear Algebra and its Applications*, 400:61–66, 2005.
- [9] G.A. Hedlund. Endomorphisms and automorphisms of the shift dynamical system. *Math. Syst. Theor.*, 3:320–375, 1969.
- [10] A. Hof and O. Knill. Cellular automata with almost periodic initial conditions. *Nonlinearity*, 8(4):477–491, 1995.
- [11] J. Jurkiewicz, R. Loll, and J. Ambjorn. Using causality to solve the puzzle of quantum spacetime. *Scientific American*, 2008.
- [12] O. Knill. A remark on quantum dynamics. *Helvetica Physica Acta*, 71:233–241, 1998.
- [13] O. Knill. On a Dehn-Sommerville functional for simplicial complexes. <https://arxiv.org/abs/1705.10439>, 2017.
- [14] O. Knill. One can hear the Euler characteristic of a simplicial complex. <https://arxiv.org/abs/1711.09527>, 2017.
- [15] O. Knill. The strong ring of simplicial complexes. <https://arxiv.org/abs/1708.01778>, 2017.
- [16] O. Knill. An elementary Dyadic Riemann hypothesis. <https://arxiv.org/abs/1801.04639>, 2018.
- [17] O. Knill. Listening to the cohomology of graphs. <https://arxiv.org/abs/1802.01238>, 2018.
- [18] M. Krivelevich and B Sudakov. The largest eigenvalue of sparse random graphs. *Combinatorics, Probability and Computing*, 12:61–72, 2003.
- [19] J. Li, W.C. Shiu, and W.H. Chan. The Laplacian spectral radius of some graphs. *Linear algebra and its applications*, pages 99–103, 2009.
- [20] J. Li, W.C. Shiu, and W.H. Chan. The Laplacian spectral radius of graphs. *Czechoslovak Mathematical Journal*, 60:835–847, 2010.
- [21] J.S. Li and X.D. Zhang. A new upper bound for eigenvalues of the Laplacian matrix of a graph. *Linear Algebra and Applications*, 265:93–100, 1997.
- [22] H. Minc. *Nonnegative Matrices*. John Wiley and Sons, 1988.
- [23] L. Pastur and A.Figotin. *Spectra of Random and Almost-Periodic Operators*, volume 297. Springer-Verlag, Berlin–New York, Grundlehren der mathematischen Wissenschaften edition, 1992.

OLIVER KNILL

- [24] J.Lacroix R. Carmona. *Spectral Theory of Random Schrödinger Operators*. Birkhäuser, 1990.
- [25] R. Merris R. Grone and V.S. Sunder. The Laplacian spectrum of a graph. *SIAM J. Matrix Anal. Appl.*, 11(2):218–238, 1990.
- [26] I. Rivin. Walks on groups, counting reducible matrices, polynomials and surface and free group automorphisms. *Duke Math. J.*, 142:353–379, 2008.
- [27] L. Shi. Bounds of the Laplacian spectral radius of graphs. *Linear algebra and its applications*, pages 755–770, 2007.
- [28] R. P. Stanley. A bound on the spectral radius of graphs. *Linear Algebra and its Applications*, 87:267–269, 1987.
- [29] D. Stevanovic. *Spectral Radius of Graphs*. Elsevier, 2015.
- [30] Xiao-Dong Zhang. Two sharp upper bounds for the Laplacian eigenvalues. *Linear Algebra and Applications*, 376:207–213, 2004.
- [31] H. Zhou and X. Xu. Sharp upper bounds for the Laplacian spectral radius of graphs. *Mathematical Problems in Engineering*, 2013, 2013.

DEPARTMENT OF MATHEMATICS, HARVARD UNIVERSITY, CAMBRIDGE, MA, 02138